Journal of Thermal Analysis and Calorimetry, Vol. 92 (2008) 2, 439–442

HEAT CAPACITIES OF A NETWORKED SYSTEM OF SINGLE-MOLECULE MAGNET WITH THREE-DIMENSIONAL STRUCTURE

S. Yamashita[1], *K. Hino*[1], *Y. Inoue*[1], *Y. Okada*[1], *R. Hirahara*[1], *Y. Nakazawa*[1,3]*, *H. Miyasaka*[2,3] *and M. Yamashita*[2,3]

[1]Department of Chemistry, Graduate School of Science, Osaka University, Toyonaka, Osaka 560-0043, Japan
[2]Department of Chemistry, Graduate School of Science, Tohoku University, Aramaki-Aza-Aoba, Sendai 980-8578, Japan
[3]CREST-JST, Honcho, Kawaguchi, Saitama 332-0012, Japan

A magnetic-fields dependence of heat capacity of $[Mn_5(hmp)_4(OH)_2\{N(CN)_2\}_6]2MeCN{\cdot}2THF$ (hmp=hydroxymethylpyridinate) is investigated by the thermal relaxation calorimetry technique. This compound is a three-dimensional system consisting of Mn_4 single-molecule magnet (SMM) units and Mn^{2+} ions, which are linked by the dicyanamide ligands to form a coordination network structure. A sharp peak of C_p being associated with the formation of three-dimensional long-range order is observed around 1.96 K. The thermodynamic discussion based on the magnetic entropy suggests that both SMMs and Mn^{2+} ions are involved in the formation of the anitiferromagnetic spin ordering. However, this long-range ordering is very sensitive to the external magnetic fields which work to change the magnitude of the Zeeman splitting of the SMM levels. The behavior under magnetic fields is similar to that of the two-dimensional Mn_4-network system studied previously.

Keywords: *heat capacity, Ising model, relaxation calorimetry, single-molecule magnet*

Introduction

The creation of single-molecule magnet (SMM) behavior [1–4] for example in Mn_{12} cluster has developed a new area in the condensed matter science, since they have provided qualitatively different features from the usual radical-based molecular magnets and metal complexes widely studied up to now. The SMM is a kind of nano-cluster complexes containing multiple transition metal ions. In each complex, metal ions are coupled by strong intra-cluster magnetic interactions and have an artificial high-spin ground state of which total spin number, S is in the order of $10–10^2$. The large uniaxial anisotropy expressed as $|D|/k_B S_z^2$ which originates from the spin-orbit coupling of constitution ions, makes such complex a nanometer-sized magnet like ferromagnetic nano-particles. Researches of the fundamental properties of the SMM and its possible application for example as quantum computing [5] or nano-memories [6, 7] are now in progress in both theoretical and experimental standpoints.

The SMM network compounds are linked system of SMM units through chemical ligands synthesized with a purpose of making cooperative character between large spin moments with high anisotropy. This system is first developed by Miyasaka and Clérac based on the idea to produce magnetically ordered state of huge spin moments. Nowadays, these materials are expected to give novel features originating from the local characters due to the SMM spins and assembled character like usual magnetic materials [8, 9]. The tuning of the balance between these two characters is succeeded by pressure and external magnetic fields with keeping the crystal structure. It is very interesting to consider the magnetic properties of these materials from a standpoint of chemical thermodynamics, since the spin degree of freedom inside the cluster and the inter-cluster interactions discussed in the usual magnetic materials coexist.

Miyasaka and Clérac took notice of the simplicity and wide possibility for structure formation of the Mn_4-complex unit to design networked materials. Four manganese ions in the unit are coupled with the strong inter-cluster interactions to form S=9 total spins. The Mn^{3+} gives the uniaxial anisotropy of D/k_B= –0.41 K [10]. The linkage of this unit into the sheet structure using the dicyanamide anions gives rise to a two-dimensional system consisting of Ising spins. Actually, they have reported that the S=9 spins of $[Mn_4(hmp)_6\{N(CN)_2\}_2](ClO_4)_2$ and $[Mn_4(hmp)_4Br_2(OMe)_2\{N(CN)_2\}_2]2THF{\cdot}0.5H_2O$ form an antiferromagnetic ordering state at 4.35 and 2.03 K, respectively. The thermodynamic analysis in [11] has claimed that the entropy of the doublet ground state of Mn_4 cluster is involved in the phase transition ensuring the bulk character of the spin ordering. It is also

* Author for correspondence: nakazawa@chem.titech.ac.jp

1388–6150/$20.00

Akadémiai Kiadó, Budapest, Hungary
Springer, Dordrecht, The Netherlands

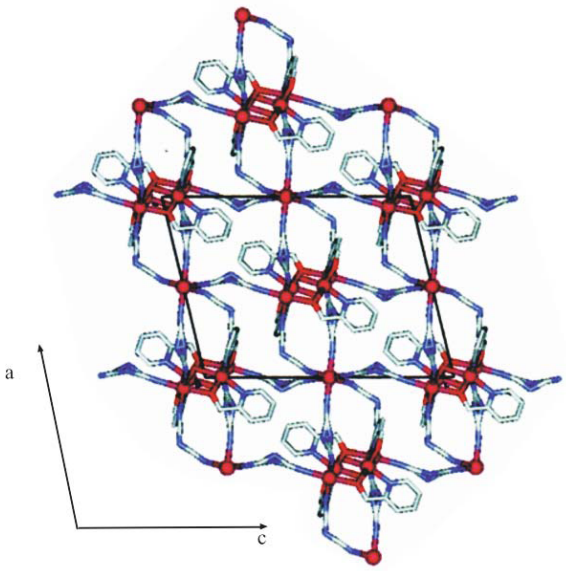

Fig. 1 The structure of three-dimensional networked system of $[Mn_5(hmp)_4(OH)_2\{N(CN)_2\}_6]2MeCN{\cdot}2THF$

interesting because the phase transition of this material is considered as the typical Ising magnet which can make a long-range order in purely 2D system. The almost symmetric peak in the heat capacity demonstrates that the magnetic order is 2D Ising type explained by the Onsager's exact solution, although the sharpness of the peak is different between two salts as is discussed in [10].

To confirm this point, the comparison with the typical 3D system consisting of the same Mn_4 units is required. Miyasaka *et al.* has synthesized the 3D network compound $[Mn_5(hmp)_4(OH)_2\{N(CN)_2\}_6]2MeCN{\cdot}2THF$ in which the same Mn_4 unit is linked through another Mn^{2+} cation as is shown in Fig. 1. The aim of this paper is to study the thermodynamic behavior of this system and discuss the thermodynamic feature of the magnetic ordering.

Experimental

We used a single crystal sample with the mass of 102.6 μg of $[Mn_5(hmp)_4(OH)_2\{N(CN)_2\}_6]2MeCN{\cdot}2THF$. This material was synthesized by Tohoku University group [12]. The crystal structure of this compound is shown in Fig. 1. The schematic illustration in Fig. 2 shows that the overall energy schemes of the Mn_4 units, determined for the typical Mn_4 cluster sample of $[Mn_4(hmp)_6\{N(CN)_2\}_2](ClO_4)_2$ from the magnetic susceptibility measurements. The ground state doublets of $S_z=\pm9$ are well isolated from the excited levels of $S_z=\pm8$.

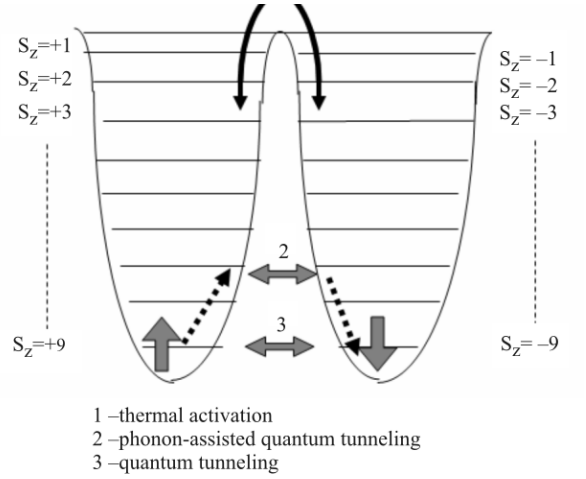

Fig. 2 The energy scheme and double well potential of single-molecule magnet system

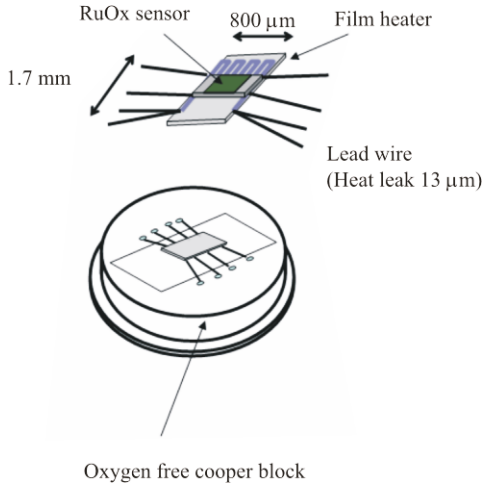

Fig. 3 The schematic illustration of the relaxation calorimetry cell

The heat capacity measurements were performed by the thermal relaxation technique developed for the single crystal measurement. The small relaxation calorimetry cell consisting of a chip type resistance of ruthenium oxide and a Ni–Cr film heater is mounted on the ^{3}He refrigerator available in the variable temperature insert (VTI) system [12, 13]. The magnetic fields were applied perpendicular to the largest surface of the plate-type crystal by the superconductive magnet. Figure 3 shows the schematic view of the calorimetric system and the sample stage. More detailed information of the calorimeter is shown in [13]. Prior to the sample measurements, we have conducted a blank measurement of the sample stage with proper amount of Apiezon N grease. The temperature dependence of the blank heat capacity is subtracted from the total heat capacity to determine the absolute value of C_p of the sample.

Results and discussion

In Fig. 4, we show temperature dependences of heat capacities of $[Mn_5(hmp)_4(OH)_2\{N(CN)_2\}_6]2MeCN{\cdot}2THF$ system in a C_pT^{-1} *vs.* T plot. The large peak is observed at 1.96 K, which is almost the similar temperature of the AF ordering of the 2D networked system of $[Mn_4(hmp)_4Br_2(OMe)_2\{N(CN)_2\}_2]2THF{\cdot}0.5H_2O$. We also show the heat capacity peak around the magnetic long-range ordered of $[Mn_4(hmp)_6\{N(CN)_2\}_2](ClO_4)_2$ system in the same figure. The heat capacities of $[Mn_5(hmp)_4(OH)_2\{N(CN)_2\}_6]2MeCN{\cdot}2THF$ system and $[Mn_4(hmp)_6\{N(CN)_2\}_2](ClO_4)_2$ system show critical behaviors around the transition temperature, but their peak-shapes are apparently different. The heat capacity peak of the former system shows a clear λ-like behavior as is observed in numerous magnetic materials, while that of the latter is almost symmetric. The difference between two compounds may be attributed to the difference of dimensionality of the magnetic interactions, since the former system is intended to construct a three-dimensional interaction between SMMs. According to the theoretical calculations of the Ising spin systems, the peak should be symmetric and the critical exponents of α, and α' gives a logarithmic divergence in the 2D case. While in the 3D Ising system, the asymmetric peak shape like λ-type anomaly is expected. The observed asymmetric peak shape which shows a sharper divergence at higher temperature side demonstrates that the phase transition of this material is expressed by the 3D Ising model. It is difficult to discuss the critical exponents from the relaxation calorimetry data, since the temperature resolution of this method is not enough to discuss the detailed structure around the transition. However, the present results demonstrate the qualitatively different character of the phase transition.

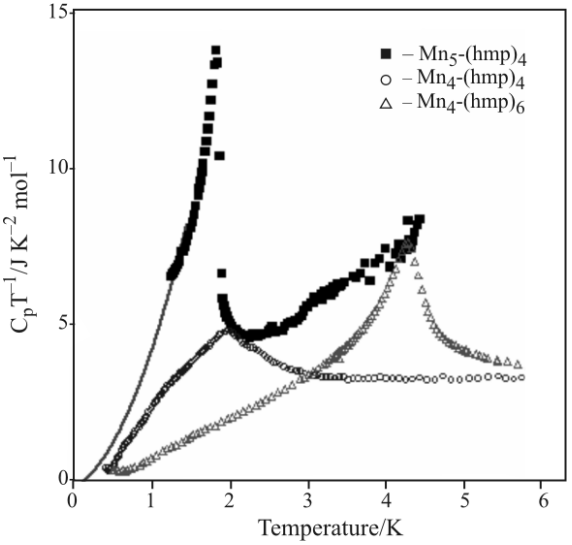

Fig. 4 Temperature dependence of heat capacity of $[Mn_5(hmp)_4(OH)_2\{N(CN)_2\}_6]2MeCN{\cdot}2THF$ (abbreviated as Mn_5-(hmp)$_4$), together with the typical 2D system of $[Mn_4(hmp)_4Br_2(OMe)_2\{N(CN)_2\}_2]2THF{\cdot}0.5H_2O$ (abbreviated as Mn_4-(hmp)$_4$) and $[Mn_4(hmp)_6\{N(CN)_2\}_2](ClO_4)_2$ (abbreviated as Mn_4-(hmp)$_6$). The solid curve demonstrates the low-temperature extrapolation of the heat capacity data based on the 3D spin-wave excitations from the antiferromagnetic ground state

The magnetic entropy of the transition is evaluated by integrating the C_pT^{-1} *vs.* T curve with respect to temperature. If the lattice heat capacity of $[Mn_5(hmp)_4(OH)_2\{N(CN)_2\}_6]2MeCN{\cdot}2THF$ should be in the similar magnitude as the Mn_4 network in 2D system expressed by the β value of 14 mJ K^{-4} mol^{-1}, the large heat capacity values observed in this plot is attributable to the magnetic correlations and Schottky heat capacity of the constituting SMMs. If we assume that the lower temperature behavior below 1.4 K where the measurement could not cover in this work is explained by the simple 3D spin wave theory of antiferromagnets, the magnetic entropy around the peak is larger than Rln2 corresponding to that of the ground state doublet of SMM. Thus, the phase transition is certainly a 3D type which involves the spins of Mn^{2+} which links the SMM units.

Temperature dependences of heat capacity under magnetic fields of the $[Mn_5(hmp)_4(OH)_2\{N(CN)_2\}_6]2MeCN{\cdot}2THF$ system are shown in Fig. 5 in a C_pT^{-1} *vs.* T plot. The magnetic fields of 0.5 and 2 T broaden the peak shape drastically and the peak temperature shift to higher temperature with the increase of magnetic fields. The broadening of the heat capacity peak by magnetic fields demonstrates that the energy levels of S_z=±9 of SMM units splits by the Zeeman energy with the increase of external magnetic fields. Taking account of the D/k_B and large S_z

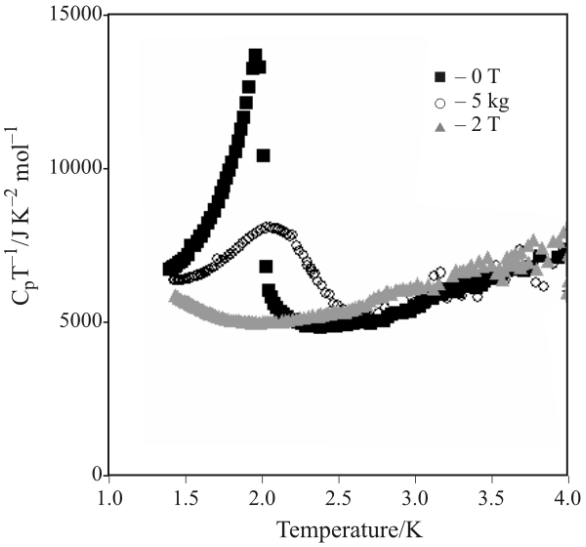

Fig. 5 The heat capacity under magnetic fields of $[Mn_5(hmp)_4(OH)_2\{N(CN)_2\}_6]2MeCN{\cdot}2THF$

value of the Mn_4 unit, a magnetic field of 0.5 T corresponds to the splitting of Δ/k_B=12 K if the Ising axis is just parallel to the external magnetic fields. Although it is difficult to adjust the Ising axis direction in the present experiments, the broadening of the peak is explained by this large Zeeman effect. Under the magnetic field of 2 T, the long-range order no longer exists and very much broadened hump which is attributable to the Schottky contribution survives in the temperature dependence of heat capacity. This feature is commonly observed in the SMM networked system for example in the preceding experiments in $[Mn_4(hmp)_6\{N(CN)_2\}_2](ClO_4)_2$ (hmp= hydroxymethylpyridinate) and $[Mn_4(hmp)_4Br_2(OMe)_2\{N(CN)_2\}_2]2THF{\cdot}0.5H_2O$. However, it should be emphasized that the tuning from 3D long-range ordering to paramagnetic state by weak magnetic fields is drastic and gives further possibility to control the magnetic state by such weak magnetic fields.

Conclusions

In summary, we have reported the result of heat capacity measurements under magnetic fields of the SMM-network material of $[Mn_5(hmp)_4(OH)_2\{N(CN)_2\}_6]2MeCN{\cdot}2THF$ where the constitutive SMM units are linked through the Mn^{2+} ions to form three-dimensional structure. The distinct peak of C_pT^{-1} which corresponds to the long-range transition at relatively high temperature as SMM systems was observed. The difference of the peak shape from those of previous 2D networked system is interpreted as the three-dimensional nature of the phase transition. The peak is drastically suppressed by applying weak magnetic fields, which means that the large Zeeman effect of each SMM unit overwhelms the inter-cluster interactions under magnetic fields.

Acknowledgements

This work was financially supported by CREST project, Japan Science and Technology Agency (JST). One of the authors YN thanks the Ikenaka Science and Technology Foundation for financial support.

References

1 G. Christou, D. Gatteschi, D. N. Hendrikson and R. Sessoli, MRS Bull., 25 (2000) 66.
2 D. Gatteschi and R. Sessoli, Angew. Chem. Int. Ed., 42 (2003) 268.
3 E. Coronado, F. Palacio and J. Veciana, Angew. Chem., Int. Ed., 42 (2003) 2570.
4 D. Gatteschi, R. Sessoli and J. Villain, 'Molecular Nanomagnets', Oxford University Press (2006).
5 M. N. Leuenberger and D. Loss, Nature, 410 (2001) 789.
6 M. R. Cheesman, V. S. Oganesyan, R. Sessoli, D. Gatteschi and A. J. Thompson, Chem. Commun., 17 (1997) 1677.
7 E. M. Chudnovsky and J. Tejada, Macroscopic Quantum Tunneling of the Magnetic Moment, Cambridge University Press, Cambridge 1998.
8 H. Miyasaka, K. Nakata, K. Sugiura, M. Yamashita and R. Clérac, Angew. Chem. Int. Ed., 43 (2004) 707.
9 H. Miyasaka and M. Yamashita, Dalton Trans., (2007) 399.
10 H. Miyasaka, K. Nakata, L. Lecren, C. Coulon, Y. Nakazawa, T. Fujisaki, K. Sugiura, M. Yamashita and R. Clérac, J. Am. Chem. Soc., 128 (2006) 3770.
11 T. Fujisaki, Y. Nakazawa, M. Oguni, K. Nakata, M. Yamashita, L. Lecren and H. Miyasaka, J. Phys. Soc. Jpn., (2007) in press.
12 M. Sorai, Ed., Comprehensive Handbook of Calorimetry and Thermal Analysis, Wiley and Sons, (2004).
13 Y. Nakazawa, A. Kawamoto and K. Kanoda, Phys. Rev., B52 (1995) 12890.

DOI: 10.1007/s10973-007-8967-x